PERGAMON

International Journal of Solids and Structures 40 (2003) 1525–1546

INTERNATIONAL JOURNAL OF SOLIDS and STRUCTURES

www.elsevier.com/locate/ijsolstr

Mechanical behaviour of laminated composite beam by the new multi-layered laminated composite structures model with transverse shear stress continuity

M. Karama *, K.S. Afaq, S. Mistou

Laboratoire Génie de Production, Equipe CMAO, Groupe M²SF, ENIT, BP 1629, 65016 Tarbes Cedex, France

Received 19 March 2002; received in revised form 4 November 2002

Abstract

This work presents a new multi-layer laminated composite structure model to predict the mechanical behaviour of multi-layered laminated composite structures. As a case study, the mechanical behaviour of laminated composite beam (90°/0°/0°/90°) is examined from both a static and dynamic point of view. The results are compared with the model "Sinus" and finite element method studied by Abou Harb. Results show that this new model is more precise than older ones as compared to the results by the finite element method (Abaqus). To introduce continuity on the interfaces of each layer, the kinematics defined by Ossadzow was used. The equilibrium equations and natural boundary conditions are derived by the principle of virtual power. To validate the new proposed model, different cases in bending, buckling and free vibration have been considered.

Keywords: Composite; Refined model; Shear transverse; Bending; Buckling; Vibration

1. Introduction

Now composite materials are used in nearly all phases of structure work, from space craft to marine vessels, from bridges and domes on civic buildings to sporting goods. The significant increase in the use of composite materials structure calls for the development of rigorous mathematical methods capable of modelling, designing and optimising of the composite under any given set of conditions.

One of the major challenges in computational structural mechanics is the development of the advanced models and numerical techniques in order to provide efficient tools exhibiting good interior and edge solutions.

In this paper we are introducing an "exponential function" as a shear stress function; the exponential functions are found to be very much richer than trigonometric Sine and Cosine functions in their Fourier

* Corresponding author. Tel.: +33-56244-2726; fax: +33-56244-2708.
E-mail address: moussa@enit.fr (M. Karama).

0020-7683/02/$ - see front matter
PII: S0020-7683(02)00647-9

Nomenclature

h	beam thickness or height
h_1	transverse shear function
H	Heaviside step function
L	beam length
m	layer number
P^*	virtual power
u_α	membrane displacement
$\ddot{U}$	differentiation w.r.t. time $= \partial^2 U/\partial t^2$
$U_{1,1}$	differentiation w.r.t. $x_1 = \partial U_1/\partial x_1$
U^*	virtual speed
w	transverse displacement
Greeks	
γ, φ_α	transverse shear rotation
ε	strain
σ	stress

development series. According to the definition of the transverse shear stress function, the existing laminated composite beam is divided into two broad categories; firstly, the global approximation models and secondly the discrete layer approximation models. The equivalent single-layer laminate theories are those in which a heterogeneous laminated plate is treated as a statically equivalent, single layer having a complex constitutive behaviour, reducing the 3D continuum problem to 2D problem.

The equivalent single layer models are:

- Kirchhoff (1850) and Love (1934) present their theory (or classical theory) in which deformation due to transverse shear is neglected, implies that the normal to the mid-plane remains straight and normal at mid-surface after deformation. This theory can be used for thin beams;
- Reissner (1945) and Mindlin (1951) present their theory (or first order theory). That the first order deformation theory extends the kinematics of the classical laminated plate theory by including a gross transverse shear deformation in its kinematic assumption, the transverse shear strain remain constant with respect to the thickness coordinate, implies that the normal to the mid-plane remains straight but not normal to mid-surface after deformation due to shear effect. The first order theory requires shear correction factors, which are difficult to determine for arbitrary laminated composite plate;
- and the higher order models are based on the hypothesis of non-linear stress variation through thickness (Reddy, 1984; Touratier, 1991). These models are able to represent the section warping in the deformed configuration.

However, these theories do not satisfy the continuity conditions of transverse shear stress at layer interfaces. Although the discrete layer approximation theories are accurate, but they are rather complex in solving problems because the order of their governing equations depends on the number of layers.

Di Sciuva (1987, 1993) and then Touratier (1991, 1992) proposed simplified discrete layer model with only five variational unknowns (two membrane displacements, a transverse displacement and two rotations), allowing the section to be represented wrapping in the deformed configuration for the Touratier (1992) model. Nevertheless, in these two cases the compatibility conditions, both layer interfaces and the

boundaries, cannot be satisfied. From Touratier's work, (Beakou, 1991) and (Idlbi, 1995) proposed, respectively, shell and plate models which satisfy both the stress continuity at interfaces and the zero stress conditions at the boundaries.

Finally, He (1994) introduced the Heaviside step function which enables automatic satisfaction of the displacement continuity at interfaces between different layers. The new discrete layer model presented comes from the work of Di Sciuva (1993), He (1994) and Ossadzow et al. (1995), the displacement field is:

$$\begin{cases} U_1(x_1,x_3,t) = u_1^0(x_1,t) - x_3 w_{,1}(x_1,t) + h_1(x_3)\phi_1(x_1,t) \\ U_2 = 0 \\ U_3(x_1,t) = w(x_1,t) \end{cases} \tag{1}$$

with transverse shear function:

$$h_1(x_3) = g(x_3) + \sum_{m=1}^{N-1} \lambda_1^{(m)} \left[\frac{-x_3}{2} + \frac{f(x_3)}{2} + (x_3 - x_3^{(m)}) H(x_3 - x_3^{(m)}) \right] \tag{2}$$

where, $H(x_3 - x_3^{(m)})$, the Heaviside Step function is defined as:

$$H(x_3 - x_3^{(m)}) = \begin{cases} 1 & \text{for } x_3 \geqslant x_3^{(m)} \\ 0 & \text{for } x_3 < x_3^{(m)} \end{cases} \tag{3}$$

and $f(x_3)$ is the shear refinement function, and $g(x_3)$ is the membrane refinement function, and the $\lambda_I^{(m)}$ are coefficients of the continuity.

New multi-layered laminated composite structures model (''KAM''):

In this work a new multi-layered laminated composite structure model is presented by using exponential function as:

$$\begin{aligned} f(z) &= z\mathrm{e}^{-2(z/h)^2} \\ g(z) &= -z\mathrm{e}^{-2(z/h)^2} \end{aligned} \tag{4}$$

for a multi-layered beam Ω, of uniform thickness 'h' and Ω is referred to the co-ordinate system $R = (0/x_1, x_2, x_3 = z)$ with z being normal to the plate's mid-surface Σ, Γ is the frontier of Ω. Then, the domain Ω is such that:

$$\Omega \subset R^3, \quad \Omega = \left\{ \Sigma \times \left[-\frac{h}{2}, \frac{h}{2} \right]; -\frac{h}{2} \leqslant z \leqslant \frac{h}{2} / M(x_1,x_2,z) \in \Omega, M_0(x_1,x_2,0) \in \Sigma, \phi \gg \mathrm{Max}(z) \right\}$$

where ϕ is the diameter of the Ω. and the closed domain $\ddot{\Omega}$ is set such that:

$$\ddot{\Omega} = \left\{ \Omega \cup \Gamma / \Gamma = \Gamma_{\text{edge}} \cup \Gamma_{z=\pm h/2} \right\}$$

From the beginning our objective was so clear, to find out a transverse shear stress function $f(z)$, which gives the mechanical behaviour of the composite laminated structures as much close as possible to the exact 3D solution by Pagano (1970) or finite element analysis in 2D (stress, strain plane), and better representation of the transverse shear stress in the thickness of the laminated structure. Since different higher order polynomial and trigonometric function already has been tried which are as follow;

Ambartsumian (1958) where;

$$f(z) = \frac{z}{2}\left[\frac{h^2}{4} - \frac{z^2}{3} \right]$$

Kaczkowski (1968), Panc (1975) and Reissner (1975) where;

$$f(z) = \frac{5}{4} z \left[1 - \frac{4z^2}{3h^2} \right]$$

Levinson (1980), Murthy (1981) and Reddy (1984) where;

$$f(z) = z \left[1 - \frac{4z^2}{3h^2} \right]$$

and finally Touratier (1991), where;

$$f(z) = \frac{h}{\pi} \sin\left(\frac{\pi z}{h} \right)$$

So, we took a start with an exponential function, because an exponential function has all even and odd power in its expansion unlike Sine function, which have only odd power. So an exponential function is much richer than a Sine function. If we take a look on the expansions of different transverse shear stress functions as;

Reddy (1984):

$$f(z) = z\left(1 - \frac{4z^2}{3h^2} \right) = z - 1.33 \frac{z^3}{h^2}$$

Touratier (1991):

$$f(z) = \frac{h}{\pi} \sin\left(\frac{\pi z}{h} \right) = z - 1.645 \frac{z^3}{h^2} + 0.812 \frac{z^5}{h^4} - 0.191 \frac{z^7}{h^6} + 0.0261 \frac{z^9}{h^8}$$

Present model:

$$f(z) = z \mathrm{e}^{-2(z/h)^2} = z - 2 \frac{z^3}{h^2} + 2 \frac{z^5}{h^4} - 1.333 \frac{z^7}{h^6} + 0.666 \frac{z^9}{h^8}$$

As it is clear from expansions of the transverse shear stress functions, that the coefficient of successive terms in 'Sine' functions are decreasing more rapidly than present exponential function which are the main responsible to gives different mechanical behaviour of laminated structures.

For the transverse shear stress behaviour, it is very important that the first derivative of the transverse shear stress function must give a parabolic response in the thickness direction of the laminate and satisfy the boundary conditions.

2. Governing equations

From the virtual power principle, the equations of motion and the natural boundary conditions can be obtained. The calculations are made in small perturbations. According to the principle of virtual power:

$$P^*_{(\mathrm{a})} = P^*_{(\mathrm{i})} + P^*_{(\mathrm{e})} \tag{5}$$

But the virtual power of the acceleration quantities are:

$$P^*_{(\mathrm{a})} = \int_\Omega \rho U^{*\mathrm{T}} \ddot{U} \, \mathrm{d}\Omega \tag{6}$$

we suppose:

$$\begin{aligned} I_w &= \int_{-h/2}^{h/2} \rho \, \mathrm{d}x_3, \quad I_{uw'} = -\int_{-h/2}^{h/2} \rho x_3 \, \mathrm{d}x_3 \\ I_{w'} &= \int_{-h/2}^{h/2} \rho x_3^2 \, \mathrm{d}x_3, \quad I_{u\omega} = \int_{-h/2}^{h/2} \rho h_1(x_3) \, \mathrm{d}x_3 \\ I_{\omega} &= \int_{-h/2}^{h/2} \rho h_1^2(x_3) \, \mathrm{d}x_3, \quad I_{\omega w'} = -\int_{-h/2}^{h/2} \rho x_3 h_1(x_3) \, \mathrm{d}x_3 \end{aligned} \tag{7}$$

so, Eq. (6) becomes (see Appendix A for the mathematical detail):

$$P^*_{(\mathrm{a})} = \int_0^L (\Gamma^{(u)} u_1^{0*} + \Gamma^{(w)} w^* + \Gamma^{(\phi)} \phi_1^*) \, \mathrm{d}x_1 + \overline{\Gamma}^{(w)} w^* \tag{8}$$

with,

$$\begin{aligned} \Gamma^{(u)} &= I_w \ddot{\boldsymbol{u}}_1^0 + I_{uw'} \ddot{\boldsymbol{w}}_{,1} + I_{u\omega} \ddot{\boldsymbol{\phi}}_1 \\ \Gamma^{(w)} &= -I_{uw'} \ddot{\boldsymbol{u}}_{1,1}^0 + I_w \ddot{\boldsymbol{w}} - I_{w'} \ddot{\boldsymbol{w}}_{,11} - I_{\omega w'} \ddot{\boldsymbol{\phi}}_{1,1} \\ \Gamma^{(\phi)} &= I_{u\omega} \ddot{\boldsymbol{u}}_1^0 + I_{\omega w'} \ddot{\boldsymbol{w}}_{,1} + I_{\omega} \ddot{\boldsymbol{\phi}}_1 \\ \overline{\Gamma}^{(w)} &= I_{uw'} \ddot{\boldsymbol{u}}_1^0 + I_{w'} \ddot{\boldsymbol{w}}_{,1} + I_{\omega w'} \ddot{\boldsymbol{\phi}}_1 \end{aligned} \tag{9}$$

Now the virtual power of internal work is:

$$P^*_{(\mathrm{i})} = \int_{\Omega} \overline{\overline{D}}^{*\mathrm{T}} : \overline{\overline{\sigma}} \, \mathrm{d}\Omega \tag{10}$$

but,

$$\overline{\overline{D}} = \begin{vmatrix} D_{11} & D_{12} & D_{13} \\ D_{21} & D_{22} & D_{23} \\ D_{31} & D_{32} & D_{33} \end{vmatrix}, \quad \overline{\overline{\sigma}} = \begin{vmatrix} \sigma_{11} & \sigma_{12} & \sigma_{13} \\ \sigma_{21} & \sigma_{22} & \sigma_{23} \\ \sigma_{31} & \sigma_{32} & \sigma_{33} \end{vmatrix}$$

so, in two dimension:

$$\overline{\overline{D}} : \overline{\overline{\sigma}} = D_{11}\sigma_{11} + 2D_{13}\sigma_{13} \tag{11}$$

Resulting stresses $N_{\alpha\beta}$, $M_{\alpha\beta}$ and $P_{\alpha\beta}$ are defined as;

$$\begin{aligned} N_{11} &= \int_{-h/2}^{h/2} \sigma_{11} \, \mathrm{d}x_3, \quad M_{11} = \int_{-h/2}^{h/2} x_3 \sigma_{11} \, \mathrm{d}x_3 \\ P_{11} &= \int_{-h/2}^{h/2} h_1(x_3) \sigma_{11} \, \mathrm{d}x_3, \quad P_{13} = \int_{-h/2}^{h/2} h_{1,3}(x_3) \sigma_{13} \, \mathrm{d}x_3 \end{aligned} \tag{12}$$

so Eq. (10) becomes (see Appendix B for the mathematical detail),

$$P^*_{(\mathrm{i})} = \int_0^L (N_{11,1} u_1^{0*} + M_{11,11} w^* + (P_{11,1} - P_{13}) \phi_1^*) \, \mathrm{d}x_1 - N_{11} u_1^{0*} - M_{11,1} w^* + M_{11} w^*_{,1} - P_{11} \phi_1^* \tag{13}$$

Now the virtual power of external loading is;

$$P^*_{(\mathrm{e})} = \int_{\Omega} U^{*\mathrm{T}} \cdot f \, \mathrm{d}\Omega + \int_{\Gamma} U^{*\mathrm{T}} \cdot \hat{F} \, \mathrm{d}\Gamma \tag{14}$$

but,

$$U^{*\mathrm{T}} = [\, U_1^* \quad 0 \quad U_3^* \,], \quad f = \begin{bmatrix} f_1 \\ f_2 \\ f_3 \end{bmatrix}, \quad F = \begin{bmatrix} F_1 \\ F_2 \\ F_3 \end{bmatrix}$$

with,

$$\begin{aligned} U_1^* &= u_1^{0*} - x_3 w_{,1}^* + h_1(x_3)\phi_1^* \\ U_2^* &= 0 \\ U_3^* &= w^* \end{aligned}$$

we define;

$$\begin{aligned} \bar{\boldsymbol{n}}_i &= \int_{-h/2}^{h/2} f_i \,\mathrm{d}x_3, \quad \overline{N}_i = \int_{-h/2}^{h/2} F_i \,\mathrm{d}x_3 \\ \bar{\boldsymbol{m}}_i &= \int_{-h/2}^{h/2} x_3 f_i \,\mathrm{d}x_3, \quad \overline{M}_i = \int_{-h/2}^{h/2} x_3 F_i \,\mathrm{d}x_3 \\ \bar{\boldsymbol{p}}_i &= \int_{-h/2}^{h/2} h_1(x_3) f_i \,\mathrm{d}x_3, \quad \overline{P}_i = \int_{-h/2}^{h/2} h_1(x_3) F_i \,\mathrm{d}x_3 \end{aligned} \tag{15}$$

so Eq. (14) becomes (see Appendix C for the mathematical detail),

$$P_{(\mathrm{e})}^* = \int_0^L (\bar{\boldsymbol{n}}_1 u_1^{0*} + (\bar{\boldsymbol{n}}_3 + \bar{\boldsymbol{m}}_{1,1}) w^* + \bar{\boldsymbol{p}}_1 \phi_1^*) \,\mathrm{d}x_1 + \overline{N}_1 u_1^{0*} (\overline{N}_3 - \bar{\boldsymbol{m}}_1) w^* - \overline{M}_1 w_{,1}^* + \overline{P}_1 \phi_1^* \tag{16}$$

Now, by Eqs. (5), (8), (13) and (16), governing equations and natural boundary conditions for $\forall u_1^{0*}$, $\forall w^*$, $\forall \phi_1^*$:

$$\begin{aligned} \Gamma^{(u)} &= N_{11,1} + \bar{\boldsymbol{n}}_1 \\ \Gamma^{(w)} &= M_{11,11} + (\bar{\boldsymbol{n}}_3 + \bar{\boldsymbol{m}}_{1,1}) \\ \Gamma^{(\phi)} &= P_{11,1} - P_{13} + \bar{\boldsymbol{p}}_1 \end{aligned} \tag{17}$$

And natural boundary conditions for $\forall u_1^{0*}$, $\forall w^*$, $\forall \phi_1^*$, $\forall w_{,1}^*$:

$$\begin{aligned} 0 &= -N_{11} + \overline{N}_1 \\ \overline{\Gamma}^{(w)} &= -M_{11,1} + (\overline{N}_3 - \bar{\boldsymbol{m}}_1) \\ 0 &= -P_{11} + \overline{P}_1 \\ 0 &= M_{11} - \overline{M}_1 \end{aligned} \tag{18}$$

The three-dimensional orthotropic constitutive law is:

$$\begin{Bmatrix} \sigma_{11} \\ \sigma_{22} \\ \sigma_{33} \\ \sigma_{23} \\ \sigma_{13} \\ \sigma_{12} \end{Bmatrix} = \begin{bmatrix} C_{11} & C_{12} & C_{13} & 0 & 0 & 0 \\ C_{12} & C_{22} & C_{23} & 0 & 0 & 0 \\ C_{13} & C_{23} & C_{33} & 0 & 0 & 0 \\ 0 & 0 & 0 & C_{44} & 0 & 0 \\ 0 & 0 & 0 & 0 & C_{55} & 0 \\ 0 & 0 & 0 & 0 & 0 & C_{66} \end{bmatrix} \begin{Bmatrix} \varepsilon_{11} \\ \varepsilon_{22} \\ \varepsilon_{33} \\ 2\varepsilon_{23} \\ 2\varepsilon_{13} \\ 2\varepsilon_{12} \end{Bmatrix} \tag{19}$$

The dimension x_2 is supposed unitary, and the effects of the σ_{33} are neglected, so orthotropic law (19), becomes;

$$\begin{Bmatrix} \sigma_{11} \\ \sigma_{13} \end{Bmatrix} = \begin{bmatrix} C'_{11} & 0 \\ 0 & C_{55} \end{bmatrix} \begin{Bmatrix} \varepsilon_{11} \\ 2\varepsilon_{13} \end{Bmatrix} \tag{20}$$

with,

$$\varepsilon_{11} = U_{1,1} = u^{0*}_{1,1} - x_3 w_{,11} + h_1 \phi_{1,1}, \quad 2\varepsilon_{31} = h_{1,3}\phi_1 \quad \text{and} \quad C'_{11} = \frac{C_{11}C_{33} - C_{13}^2}{C_{33}}$$

Now, the generalized constitutive law;

$$\begin{bmatrix} N_{11} \\ M_{11} \\ P_{11} \\ P_{13} \end{bmatrix} = \begin{bmatrix} A_{11} & B_{11} & \widetilde{K} & 0 \\ B_{11} & D_{11} & \widetilde{T} & 0 \\ \widetilde{K} & \widetilde{T} & \widetilde{S} & 0 \\ 0 & 0 & 0 & \widetilde{Y} \end{bmatrix} \begin{bmatrix} u^{0*}_{1,1} \\ -w_{,11} \\ \phi_{1,1} \\ \phi_1 \end{bmatrix} \tag{21}$$

so, the governing equations (17), become:

$$\begin{aligned} \Gamma^{(u)} &= A_{11}u^{0*}_{1,11} - B_{11}w_{,111} + \widetilde{K}\phi_{1,11} + \bar{n}_1 \\ \Gamma^{(w)} &= B_{11}u^{0*}_{1,111} - D_{11}w_{,1111} + \widetilde{T}\phi_{1,111} + \bar{n}_3 + \bar{m}_{1,1} \\ \Gamma^{(\phi)} &= \widetilde{K}u^{0*}_{1,11} - \widetilde{T}w_{,111} + \widetilde{S}\phi_{1,11} - \widetilde{Y}\phi_1 + \bar{p}_1 \end{aligned} \tag{22}$$

and the natural boundary conditions (18), become:

$$\begin{aligned} 0 &= A_{11}u^{0*}_{1,1} - B_{11}w_{,11} - \widetilde{K}\phi_{1,1} + \overline{N}_1 \\ \overline{\Gamma}^{(w)} &= -B_{11}u^{0*}_{1,11} + D_{11}w_{,111} - \widetilde{T}\phi_{1,11} + \overline{N}_3 - \bar{m}_1 \\ 0 &= -\widetilde{K}u^{0*}_{1,1} + \widetilde{T}w_{,11} - \widetilde{S}\phi_{1,1} + \overline{P}_1 \\ 0 &= -B_{11}u^{0*}_{1,1} - D_{11}w_{,11} + \widetilde{T}\phi_{1,1} - \overline{M}_1 \end{aligned} \tag{23}$$

Continuity coefficients (λ): To find out the value of the continuity coefficients, the conditions of the continuity of the transverse shear stress between each interfaces of the layers were used (Fig. 1);

$$\sigma^{(m)}_{13}\left(x_3 = x^{(m)}_3\right) = \sigma^{(m+1)}_{13}\left(x_3 = x^{(m)}_3\right) \tag{24}$$

Interface of layer (1) and layer (2):

$$\sigma^{(1)}_{13}\left(x_3 = x^{(1)}_3\right) = \sigma^{(2)}_{13}\left(x_3 = x^{(1)}_3\right)$$

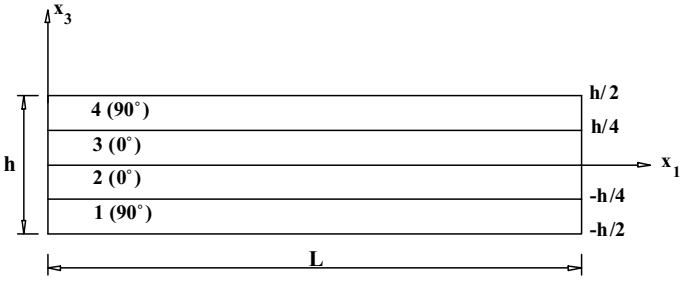

Fig. 1. Description of the beam.

$$Q_{55}^{1}\phi(x_1)\left[g'(x_3^{(1)})+(\lambda_1^{(1)}+\lambda_1^{(2)}+\lambda_1^{(3)})\left(\frac{-1}{2}+\frac{f'(x_3^{(1)})}{2}\right)\right]$$
$$=Q_{55}^{2}\phi(x_1)\left[g'(x_3^{(1)})+(\lambda_1^{(1)}+\lambda_1^{(2)}+\lambda_1^{(3)})\left(\frac{-1}{2}+\frac{f'(x_3^{(1)})}{2}\right)+\lambda_1^{(1)}\right] \tag{25}$$

Interface of layer (2) and layer (3):

$$\sigma_{13}^{(2)}\left(x_3=x_3^{(2)}\right)=\sigma_{13}^{(3)}\left(x_3=x_3^{(2)}\right)$$

Since, Q_{55} of the second and third layer are equal (Fig. 1), so,

$$Q_{55}^{2}\phi(x_1)\left[g'(x_3^{(2)})+(\lambda_1^{(1)}+\lambda_1^{(2)}+\lambda_1^{(3)})\left(\frac{-1}{2}+\frac{f'(x_3^{(2)})}{2}\right)+\lambda_1^{(1)}\right]$$
$$=Q_{55}^{3}\phi(x_1)\left[g'(x_3^{(2)})+(\lambda_1^{(1)}+\lambda_1^{(2)}+\lambda_1^{(3)})\left(\frac{-1}{2}+\frac{f'(x_3^{(2)})}{2}\right)+\lambda_1^{(1)}+\lambda_1^{(2)}\right] \tag{26}$$

Now by Eqs. (25) and (26),

$$\begin{aligned}\lambda_1^{(1)}&=\lambda_1^{(1)}+\lambda_1^{(2)}\\ \lambda_1^{(2)}&=0\end{aligned} \tag{27}$$

This shows that if the mechanical characteristics of the two consecutive layers are the same (Fig. 1), the coefficient of the continuity will be zero ($\lambda^{(2)}=0$).

Interface of layer (3) and layer (4):

$$\sigma_{13}^{(3)}(x_3=x_3^{(3)})=\sigma_{13}^{(4)}(x_3=x_3^{(3)})$$

$$Q_{55}^{3}\phi(x_1)\left[g'(x_3^{(3)})+(\lambda_1^{(1)}+\lambda_1^{(2)}+\lambda_1^{(3)})\left(\frac{-1}{2}+\frac{f'(x_3^{(3)})}{2}\right)+\lambda_1^{(1)}+\lambda_1^{(2)}\right]$$
$$=Q_{55}^{4}\phi(x_1)\left[g'(x_3^{(3)})+(\lambda_1^{(1)}+\lambda_1^{(2)}+\lambda_1^{(3)})\left(\frac{-1}{2}+\frac{f'(x_3^{(3)})}{2}\right)+\lambda_1^{(1)}+\lambda_1^{(2)}+\lambda_1^{(3)}\right] \tag{28}$$

we have,

$$f'(x_3^{(1)}=-h/4)=f'(x_3^{(3)}=h/4)\quad\text{and}\quad g'(x_3^{(1)}=-h/4)=g'(x_3^{(3)}=h/4)$$

So, by Eqs. (26)–(28), gives;

$$Q_{55}^{1}\phi(x_1)\left[g'(x_3^{(3)})+(\lambda_1^{(1)}+\lambda_1^{(2)}+\lambda_1^{(3)})\left(\frac{-1}{2}+\frac{f'(x_3^{(3)})}{2}\right)\right]$$
$$=Q_{55}^{4}\phi(x_1)\left[g'(x_3^{(3)})+(\lambda_1^{(1)}+\lambda_1^{(2)}+\lambda_1^{(3)})\left(\frac{-1}{2}+\frac{f'(x_3^{(3)})}{2}\right)+\lambda_1^{(1)}+\lambda_1^{(3)}\right]$$

$$\begin{aligned}0&=\lambda_1^{(1)}+\lambda_1^{(3)}\\ \lambda_1^{(1)}&=-\lambda_1^{(3)}\end{aligned} \tag{29}$$

So, by Eqs. (27) and (29), Eq. (25) becomes;

$$Q^1_{55}(g'(x_3^{(1)})) = Q^2_{55}(g'(x_3^{(1)}) + \lambda_1^{(1)}), \quad \lambda_1^{(1)} = \frac{(Q^1_{55} - Q^2_{55})g'(x_3^{(1)})}{Q^2_{55}} \quad \text{and} \quad \lambda_1^{(3)} = \frac{(Q^2_{55} - Q^1_{55})g'(x_3^{(1)})}{Q^2_{55}} \tag{30}$$

Finite element analysis: Since no exact 3D solution exists for the considered case study, so ABAQUS (finite element analysis software) is used to show the efficiency of the present model. In this paper finite element results are taken as a reference for the comparison of different models of laminated composite structures, done by Karama et al. (1993, 1998). The 3D approximation of the behaviour is carried out by element type "CPS8" (quadrilateral element of eight node, 16 ddl per element). To validate the finite element results, firstly it is necessary to find out the convergence of laminate meshing. So, for the given problem, in static and dynamic, the convergence found to be at 1680 elements included 24 element in thickness.

3. Some evaluations of the present model

3.1. Bending analysis

The static bending analysis is studied, so the virtual power of acceleration quantities are cancelled. Three different bending analyses have been developed for three different specific boundary conditions. For the simply supported conditions, the unknown variables are deduced directly by the equation of motions. For clamped conditions, kinematic boundary conditions are used and, finally, in a free edge case, natural boundary conditions are employed.

The beam studied has a length of $L = 6.35$ m, a unitary width, and a thickness $h = 2.794$ m in the thick case and $h = 0.2794$ m in the thin case. The beam possesses four layers of the same thickness at 90°/0°/0°/90°. The material used for the four layers is boron epoxy. The mechanical properties of the 0° layer are as follows (Widera and Logan, 1980):

$$E_{11} = 241.5 \text{ GPa} \quad E_{22} = E_{33} = 18.89 \text{ GPa} \quad G_{23} = 3.45 \text{ GPa} \quad G_{12} = G_{13} = 5.18 \text{ GPa}$$
$$\nu_{23} = 0.25 \quad \nu_{12} = \nu_{13} = 0.24$$

and the density, $\rho = 2015$ kg/m^3.

The continuity coefficients from Eqs. (27), (29) and (30):

$$\lambda_1^{(1)} = -\lambda_1^{(3)} = 0.2210501411, \quad \lambda_1^{(2)} = 0$$

Problem 1. Bending of a simply supported beam under distributed sinusoidal load.

The surface and volume force components are cancelled except:

$$\bar{n}_3 = \int_0^h f_3 \, dx_3 = q = q_0 \sin\left(\frac{\pi x_1}{L}\right)$$

For the simply supported boundary conditions, the Levy solution is used, define as;

$$u_1^0 = u_0 \cos\left(\frac{\pi x_1}{L}\right), \quad w = w_0 \sin\left(\frac{\pi x_1}{L}\right), \quad \phi_1 = \phi_0 \cos\left(\frac{\pi x_1}{L}\right) \tag{31}$$

Now the governing equations (22), with $P^*_{(a)} = 0$, becomes

$$
\begin{aligned}
0 &= A_{11}u^{0*}_{1,11} - B_{11}w_{,111} + \widetilde{K}\phi_{1,11} \\
0 &= B_{11}u^{0*}_{1,111} - D_{11}w_{,1111} + \widetilde{T}\phi_{1,111} + q_0 \sin\left(\frac{\pi x_1}{L}\right) \\
0 &= \widetilde{K}u^{0*}_{1,11} - \widetilde{T}w_{,111} + \widetilde{S}\phi_{1,11} - \widetilde{Y}\phi_1
\end{aligned} \tag{32}
$$

Now, by the Levy solution, the governing equations become;

$$
\begin{aligned}
0 &= -A_{11}\alpha^2 u_0 \cos\alpha x_1 + B_{11}\alpha^3 w_0 \cos\alpha x_1 - \widetilde{K}\alpha^2\phi_0 \cos\alpha x_1 \\
0 &= B_{11}\alpha^3 u_0 \sin\alpha x_1 - D_{11}\alpha^4 w_0 \sin\alpha x_1 + \widetilde{T}\alpha^3\phi_0 \sin\alpha x_1 + q_0 \sin\alpha x_1 \\
0 &= -\widetilde{K}\alpha^2 u_0 \cos\alpha x_1 + \widetilde{T}\alpha^3 w_0 \cos\alpha x_1 - \widetilde{S}\alpha^2\phi_0 \cos\alpha x_1 - \widetilde{Y}\phi_0 \cos\alpha x_1
\end{aligned}
$$

with,

$$
\alpha = \frac{\pi}{L}
$$

and then in matrix form,

$$
\begin{bmatrix}
-\alpha^2 A_{11} & \alpha^3 B_{11} & -\alpha^2\widetilde{K} \\
\alpha^3 B_{11} & -\alpha^4 D_{11} & \alpha^3\widetilde{T} \\
-\alpha^2\widetilde{K} & \alpha^3\widetilde{T} & -\alpha^2\widetilde{S} - \widetilde{Y}
\end{bmatrix}
\begin{pmatrix} u_0 \\ w_0 \\ \phi_0 \end{pmatrix} =
\begin{pmatrix} 0 \\ -q_0 \\ 0 \end{pmatrix} \tag{33}
$$

and also, the displacement (1), becomes;

$$
\begin{aligned}
U_1(x_1, x_3) &= (u_0 - x_3 w_0 \alpha + h_1(x_3)\phi_0)\cos(\alpha x_1) \\
U_2 &= 0 \\
U_3 &= w_0 \sin(\alpha x_1)
\end{aligned} \tag{34}
$$

Table 1
Underlining of the membrane refinement introduces in the new model in relation to the Sine model, continuous model without refinement of Idlbi (Idlbi, 1995) and Abaqus (Karama et al., 1993)

x_3	$U_1(L/2, x_3)$ (10^{-7} m)			
	Present	Sine (Karama et al., 1993)	Idlbi (Idlbi, 1995)	Abaqus (Karama et al., 1993)
$-h/2$	−7.365	−7.192	−7.116	−8.093
$-3h/8$	−4.903	−4.812	−4.756	−5.446
$-h/4$	−3.068	−3.074	−3.081	−2.998
$-h/8$	−1.373	−1.404	−1.399	−1.195
0	0	0	0	0
$h/8$	1.373	1.404	1.399	1.195
$h/4$	3.068	3.074	3.081	2.998
$3h/8$	4.903	4.812	4.756	5.446
$h/2$	7.365	7.192	7.116	8.093

Table 2
Bending of the simply supported thick beam under distributed sinusoidal load

Model	$U_3(L/2)$ (m)	$U_1(0, h/2)$ (m)	$\sigma_{13}(L/4, 0)$ (Pa)	$\sigma_{11}(L/2, -h/4^+)$ (Pa)	$\sigma_{33}(L/2, h/2)$ (Pa)
Present	-6.3701×10^{-4}	2.1196×10^{-4}	−940098.0	8112840.0	−1039990.0
Error (%)	4.4	8.3	6.6	3.5	3.9
Sine (Karama et al., 1993)	-6.2794×10^{-4}	2.0180×10^{-4}	−896865.0	8158932.0	−1047274.0
Error (%)	2.9	12.7	10.8	4.1	4.6
Abaqus (Karama et al., 1993)	-6.1006×10^{-4}	2.3125×10^{-4}	−1006000.0	7835200.0	−1000900.0

and now by relation (20), stresses expression;

$$\sigma_{11}(x_1, x_3) = -\alpha C'_{11}(u_0 - \alpha x_3 w_0 + h_1 \phi_0) \sin(\alpha x_1) \tag{35}$$

and,

$$\sigma_{13}(x_1, x_3) = C_{55} h_{1,3} \phi_0 \cos(\alpha x_1) \tag{36}$$

and integration of the equilibrium equation $\sigma_{13,1} + \sigma_{33,3} = 0$, enables us to calculate the analytical value of σ_{33};

$$\sigma_{33} = \alpha C_{55} h_1(x_3) \phi_0 \sin(\alpha x_1) \tag{37}$$

The numerical results obtained ($q_0 = -10^6$ Pa) using the present model are compared with those obtained by: the finite element analysis (Karama et al., 1993) and the Sine (Karama et al., 1993) model by Touratier (1991). For this problem, the present model is better than Sine model as compared to the finite element analysis results, except the transverse deflection (U_3). Percentage error reduction is more significant in case of transverse shear stress (σ_{13}) (Tables 1 and 2).

The efficiency of this model is shown for (Figs. 2–4), different stresses and displacement plotted according to the length and thickness of the beam, showing that the present model at every point on the beam,

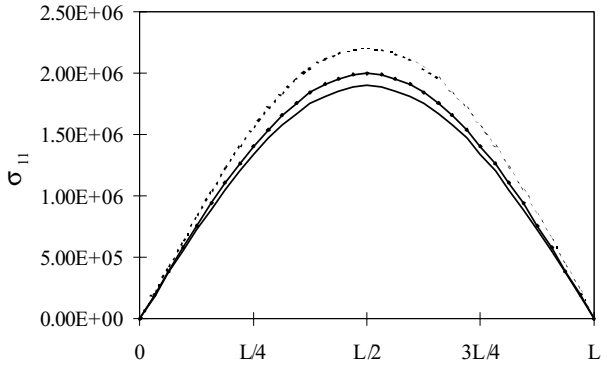

Fig. 2. Variation of the stress σ_{11} along the direction x_1 for $x_3 = -h/2$ for Problem 1. Present (-∗-), Sine (Karama et al., 1993) (–), Abaqus (Karama et al., 1993) (- - -).

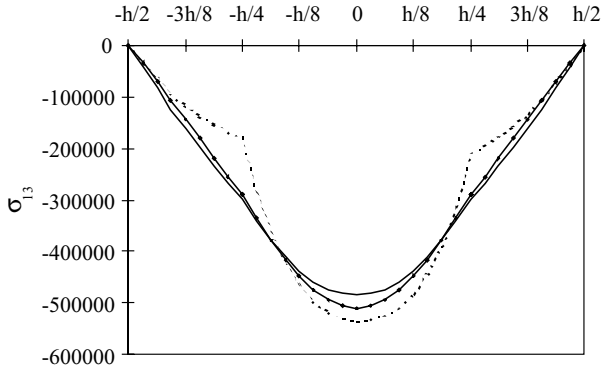

Fig. 3. Variation of the stress σ_{13} through the thickness for $x_1 = 3L/8$ for Problem 1. Present (-∗-), Sine (Karama et al., 1993) (–), Abaqus (Karama et al., 1993) (- - -).

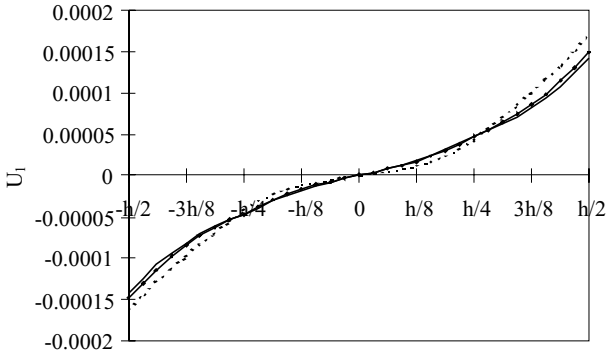

Fig. 4. Variation of the displacement U_1 through the thickness for $x_1 = L/4$ for Problem 1. Present (-∗-), Sine (Karama et al., 1993) (–), Abaqus (Karama et al., 1993) (- - -).

is closer to the finite element results then to those of the Sine model. Here we can see also the continuity of displacement and transverse shear stress between layer interfaces of the present model.

Problem 2. Bending of a clamped free beam under distributed uniform load.

In this case the value of $\bar{n}_3$ is:

$$\bar{n}_3 = \int_{-h/2}^{h/2} f_3 \, \mathrm{d}x_3 = q \tag{38}$$

Now, the governing equation from system of equations (22),

$$\begin{aligned} 0 &= A_{11} u^{0*}_{1,11} - B_{11} w_{,111} + \widetilde{K} \phi_{1,11} \\ 0 &= B_{11} u^{0*}_{1,111} - D_{11} w_{,1111} + \widetilde{T} \phi_{1,111} + q \\ 0 &= \widetilde{K} u^{0*}_{1,11} - \widetilde{T} w_{,111} + \widetilde{S} \phi_{1,11} - \widetilde{Y} \phi_1 \end{aligned} \tag{39}$$

by integration and simultaneously solving the above equations, gives;

$$\begin{aligned} \phi_1(x_1) &= C_1 \mathrm{e}^{-Px_1} + C_2 \mathrm{e}^{Px_1} - (qx_1 + C_3) \frac{\widetilde{T}}{\widetilde{Y} D_{11}} \\ u^0_1(x_1) &= -\frac{\widetilde{K}}{A_{11}} \phi_1(x_1) + C_7 x_1 + C_8 \\ w(x_1) &= \frac{\widetilde{T}}{P D_{11}} \left[C_1 \mathrm{e}^{-Px_1} + C_2 \mathrm{e}^{Px_1} - \left(\frac{q x_1^2}{2} + C_3 x_1 \right) \frac{P}{\widetilde{Y}} \right] + \frac{1}{D_{11}} \left(\frac{q x_1^4}{24} + C_3 \frac{x_1^3}{6} \right) + C_4 \frac{x_1^2}{2} + C_5 x + C_6 \end{aligned}$$

with

$$P = \sqrt{\frac{-\widetilde{Y} A_{11} D_{11}}{\widetilde{K}^2 D_{11} + \widetilde{T}^2 A_{11} - \widetilde{S} A_{11} D_{11}}} \tag{40}$$

and $(B_{11} = 0)$ due to the symmetry about mid-surface. Eight constant C_i are determined by the four natural boundary conditions at the free edge deduced from (23) with $P^*_{(a)} = 0$:

$$0 = A_{11}u^{0*}_{1,1}(L) - \widetilde{K}\phi_{1,1}(L)$$
$$0 = D_{11}w_{,111}(L) - \widetilde{T}\phi_{1,11}(L)$$
$$0 = -\widetilde{K}u^{0*}_{1,1}(L) + \widetilde{T}w_{,11}(L) - \widetilde{S}\phi_{1,1}(L)$$
$$0 = -D_{11}w_{,11}(L) + \widetilde{T}\phi_{1,1}(L)$$

and by the four kinematics boundary conditions at clamped edge:

$$u^0_1(0) = 0, \quad w(0) = 0, \quad w_{,1}(0) = 0, \quad \phi_1(0) = 0$$

The numerical results (Table 3), obtained ($q = -1000$ N/m) using the present model for the same beam as in Problem 1, except for the load now being uniformly distributed instead of *sinusoidal,* show that the present model still has less percentage of error as compared to the Sine model. In this case, the displacements are closer to the numerical result given by Abaqus as compared to the Sine model. In (Figs. 5–7), different stresses and displacement are plotted according to the length and thickness of the beam, showing the difference between the present model and Sine model as regards the finite element. The present model is in close agreement with the Abaqus results.

Problem 3. Bending of a clamped free beam under concentrated load.

In this case the value of $\overline{N}_3$ is:

$$\overline{N}_3 = \int_{-h/2}^{h/2} F_3 \, \mathrm{d}x_3 = q \tag{41}$$

Table 3
Bending of a clamped/free thick beam under uniformly distributed load

Model	$U_3(L)$ (m)	$U_1(L/2, h/2)$ (m)	$\sigma_{13}(L/4, 0)$ (Pa)	$\sigma_{11}(L/2, -h/4^+)$ (Pa)	$\sigma_{33}(L/2, h/2)$ (Pa)
Present	-4.40057×10^{-6}	7.36497×10^{-7}	−3181.03	−9986.18	−1067.1
Error (%)	2.6	9.8	−2.3	7.9	−4.3
Sine (Karama et al., 1993)	-4.37885×10^{-6}	7.19163×10^{-7}	−3031.42	−9939.3	−1066.64
Error (%)	3.1	11.9	2.5	8.3	−4.3
Abaqus (Karama et al., 1993)	-4.51810×10^{-6}	8.16300×10^{-7}	−3110.0	−10842.0	−1023.0

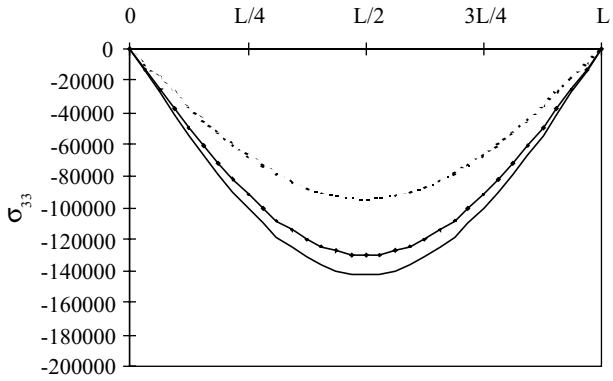

Fig. 5. Variation of the stress σ_{33} along the direction x_1 for $x_3 = h/4^+$ for Problem 1. Present (-∗-), Sine (Karama et al., 1993) (–), Abaqus (Karama et al., 1993) (- - -).

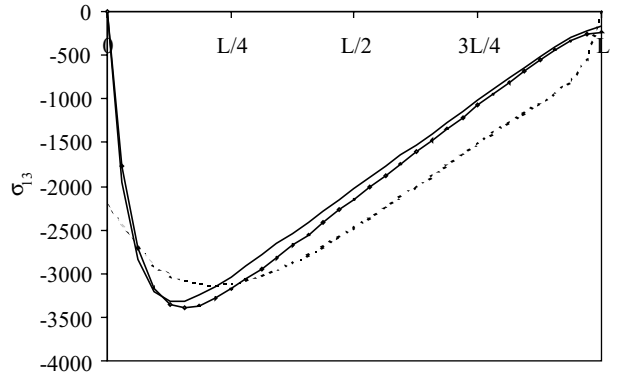

Fig. 6. Variation of the stress σ_{13} along the direction x_1 for $x_3 = 0$ for Problem 2. Present (-∗-), Sine (Karama et al., 1993) (–), Abaqus (Karama et al., 1993) (- - -).

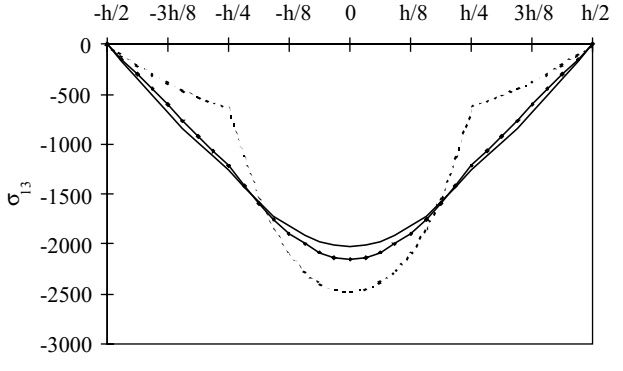

Fig. 7. Variation of the stress σ_{13} through the thickness for $x_1 = L/2$. for Problem 2. Present (-∗-), Sine (Karama et al., 1993) (–), Abaqus (Karama et al., 1993) (- - -).

Now, the governing equation from the system of equations (22),

$$\begin{aligned} 0 &= A_{11}u^{0*}_{1,11} - B_{11}w_{,111} + \widetilde{K}\phi_{1,11} \\ 0 &= B_{11}u^{0*}_{1,111} - D_{11}w_{,1111} + \widetilde{T}\phi_{1,111} \\ 0 &= \widetilde{K}u^{0*}_{1,11} - \widetilde{T}w_{,111} + \widetilde{S}\phi_{1,11} - \widetilde{Y}\phi_1 \end{aligned} \tag{42}$$

by integration and simultaneous solving of the above equations, gives;

$$\phi_1(x_1) = C_1 e^{-Px_1} + C_2 e^{Px_1} - C_3 \frac{\widetilde{T}}{\widetilde{Y}D_{11}},$$

$$u^0_1(x_1) = -\frac{\widetilde{K}}{A_{11}}\phi_1(x_1) + C_7 x_1 + C_8,$$

$$w(x_1) = \frac{\widetilde{T}}{PD_{11}}\left[C_1 e^{-Px_1} + C_2 e^{Px_1} - C_3 x_1 \frac{P}{\widetilde{Y}}\right] + \frac{C_3}{D_{11}}\frac{x_1^3}{6} + C_4\frac{x_1^2}{2} + C_5 x + C_6$$

with

$$P = \sqrt{\frac{-\widetilde{Y}A_{11}D_{11}}{\widetilde{K}^2D_{11} + \widetilde{T}^2A_{11} - \widetilde{S}A_{11}D_{11}}} \tag{43}$$

and ($B_{11} = 0$) due to the symmetry about mid-surface. Eight constant C_i are determined by the four natural boundary conditions at the free edge deduced from (23) with $P^*_{(a)} = 0$:

$$\begin{aligned}
0 &= A_{11}u^{0*}_{1,1}(L) - \widetilde{K}\phi_{1,1}(L)\\
0 &= -D_{11}w_{,111}(L) + \widetilde{T}\phi_{1,11}(L) - q\\
0 &= -\widetilde{K}u^{0*}_{1,1}(L) + \widetilde{T}w_{,11}(L) - \widetilde{S}\phi_{1,1}(L)\\
0 &= -D_{11}w_{,11}(L) + \widetilde{T}\phi_{1,1}(L)
\end{aligned}$$

and by the four kinematics boundary conditions at the clamped edge:

$$u^0_1(0) = 0, \quad w(0) = 0, \quad w_{,1}(0) = 0, \quad \phi_1(0) = 0$$

The numerical results (Table 4), obtained ($q = -10{,}000$ N) using the present model for the same beam as in Problem 2 except that loading is now concentrated at the free end of the beam, our reference still being the Abaqus results (Karama et al., 1993), show that the present model still has very good results compared to the Sine model except with regard to membrane stress (σ_{11}) where no difference was found.

3.2. Buckling analysis

The analysis of the buckling behaviour underlines a succession of the stable equilibrium configurations in a plane stress state. This fundamental equilibrium trajectory is followed by the structure from the loading. Then there is a critical point where the equilibrium losses its stability; this is the buckling critical load (Gachon, 1980) and (Palardy and Palazotto, 1990).

Problem 4. Buckling of a simply supported thin beam.

The buckling is a non-linear static problem with large displacements. The ε_{11} strain is composed of a linear part and a non-linear part (Widera and Logan, 1980): $\varepsilon_{11} = U_{1,1} + (1/2)(w_{,1})^2$.

The non-linear term modifies the value of the virtual power of the internal work as follows:

$$\begin{aligned}
P^*_{(i)} &= P^{*L}_{(i)} + P^{*NL}_{(i)}\\
P^*_{(i)} &= -\int_\Omega \sigma_{11}w_{,11}w^*\,d\Omega = \int_0^L N^0_{11}w_{,11}w^*\,dx_1 - N^0_{11}w_{,1}w^*
\end{aligned} \tag{44}$$

Table 4
Bending of a clamped/free thick beam under concentrated load

Model	$U_3(L)$ (m)	$U_1(L/2, h/2)$ (m)	$\sigma_{13}(L/4, 0)$ (Pa)	$\sigma_{11}(L/2, -h/4^+)$ (Pa)
Present	-1.67021×10^{-5}	2.87160×10^{-6}	−6699.43	−62969.5
Error (%)	0.1	8.8	4.7	−1.4
Sine (Karama et al., 1993)	-1.65722×10^{-5}	2.81698×10^{-6}	−6372.07	−62969.5
Error (%)	0.8	10.5	9.3	−1.4
Abaqus (Karama et al., 1993)	-1.67110×10^{-5}	3.14800×10^{-6}	−7027.0	−62091.0

with

$$N_{11}^0 = \int_{-h/2}^{h/2} \sigma_{11}^0 \, dx_3 = \text{compression load}$$

The equilibriums in Eqs. (22) are modified by the non-linear terms:

$$\begin{aligned} 0 &= A_{11} u_{1,11}^{0*} - B_{11} w_{,111} + \widetilde{K} \phi_{1,11} \\ 0 &= B_{11} u_{1,111}^{0*} - D_{11} w_{,1111} + \widetilde{T} \phi_{1,111} + N_{11}^0 w_{,11} \\ 0 &= \widetilde{K} u_{1,11}^{0*} - \widetilde{T} w_{,111} + \widetilde{S} \phi_{1,11} - \widetilde{Y} \phi_1 \end{aligned} \tag{45}$$

The Levy type solution supposes u_1^0, w and ϕ_1 as follows:

$$u_1^0 = U_n \cos \psi_n x_1, \quad w = W_n \sin \psi_n x_1, \quad \phi_1 = \phi_n \cos \psi_n x_1,$$

with

$$\psi_n = \left(\frac{n\pi}{L} \right)$$

where n is an integer. To determine the critical buckling load, the value of N_{11}^0 found has to cancel the determinant of the system (45). By changing the n, for the different buckling modes, the different critical loads can be obtained, giving;

$$N_{11C}^0 = -N_{11}^0 = \psi_n^2 \left[D_{11} - \frac{\psi_n^2 (2\widetilde{K} B_{11} \widetilde{T} - A_{11} \widetilde{T}^2 - B_{11}^2 \widetilde{S}) - B_{11}^2 \widetilde{Y}}{\psi_n^2 (\widetilde{K}^2 - A_{11} \widetilde{S}) - A_{11} \widetilde{Y}} \right] \tag{46}$$

In (Table 5), the critical buckling load is calculated for different modes of buckling using the present model. Until six mode of buckling, there is no difference has found between present and Sine model as compare to numerical results by Abaqus (Karama et al., 1993). After sixth mode of buckling, results by both models diverge progressively with same percentage of error.

3.3. Free vibration analysis

The dynamic analysis is realised in the free vibration case. All the terms of the motion equation (22) are taken into account. Two studies in free vibration, with and without initial load are developed. In each problem this concerns simply supported thick and thin beams. The surface and volume components are cancelled in two studies.

Table 5
Critical loads for the buckling of a simply supported thin beam for the first six modes

N	N_{11C}^0 (N)—Present	Error (%)	N_{11C}^0 (N)—Sine (Karama et al., 1993)	Error (%)	N_{11C}^0 (N)—Abaqus (Karama et al., 1993)
1	20362279.35	0.09	20362280.0	0.09	20381400.0
2	76428157.72	−0.03	76428160.0	−0.03	76407200.0
3	155963320.2	0.56	155963320.0	0.56	156844000.0
4	245376869.5	2.17	245376870.0	2.17	250822000.0
5	334136061.5	4.69	334136060.0	4.69	350573000.0
6	416057469.7	7.80	416057470.0	7.80	451275000.0

Problem 5. Free vibration without an initial load.

The equation system is deduced from equations of motions (22):

$$\begin{aligned}\Gamma^{(u)} &= A_{11}u^{0*}_{1,11} - B_{11}w_{,111} + \widetilde{K}\phi_{1,11}\\ \Gamma^{(w)} &= B_{11}u^{0*}_{1,111} - D_{11}w_{,1111} + \widetilde{T}\phi_{1,111}\\ \Gamma^{(\phi)} &= \widetilde{K}u^{0*}_{1,11} - \widetilde{T}w_{,111} + \widetilde{S}\phi_{1,11} - \widetilde{Y}\phi_1\end{aligned} \tag{47}$$

The Levy type solution supposes:

$$\begin{aligned}u^0_1 &= U_n\cos(\psi_n x_1)\exp(\mathrm{i}\omega t)\\ w &= W_n\sin(\psi_n x_1)\exp(\mathrm{i}\omega t)\\ \phi_1 &= \Phi_n\cos(\psi_n x_1)\exp(\mathrm{i}\omega t)\end{aligned} \tag{48}$$

with $\psi_n = n\pi/L$, n is an integer for the number of mode.

To determine the vibration frequency, the determinant of the system of equation (47) equals zero:

$$\begin{bmatrix} I_w\omega^2 - \psi_n^2 A_{11} & I_{uw'}\psi_n\omega^2 + \psi_n^3 B_{11} & I_{u\omega}\omega^2 - \psi_n^2\widetilde{K}\\ I_{uw'}\psi_n^2\omega^2 + \psi_n^3 B_{11} & I_w\omega^2 + I_{w'}\psi_n^2\omega^2 - \psi_n^4 D_{11} & I_{\omega w'}\psi_n\omega^2 + \psi_n^3\widetilde{T}\\ I_{u\omega}\omega^2 - \psi_n^2\widetilde{K} & I_{\omega w'}\psi_n\omega^2 + \psi_n^3\widetilde{T} & I_\omega\omega^2 - \psi_n^2\widetilde{S} - \widetilde{Y}\end{bmatrix}\begin{pmatrix} U_n\\ W_n\\ \Phi_n\end{pmatrix} = 0 \tag{49}$$

So, now for different values of n, different equation are obtained, in which the smallest positive root gives the vibration frequency of associated mode n.

In (Tables 6 and 7), results are presented for the free vibration of thin and thick beams respectively. For different modes of vibration, frequencies are calculated using the present model. In the case of the thin beam, frequencies are found to be very close to Abaqus, as far as the 10th mode of vibration, compared to the Sine model, but after the 10th mode, results diverge compared to the Sine model. However there is no big difference of error between the two models, the maximum error obtained with the present model is less than 0.9%, and 1.5% with the Sine model as far as the 12th mode of vibration.

In the case of the thick beam, the results are more or less unfavourable with the present model compared to the Sine model. However, frequencies diverge very rapidly after the 5th mode compare to the Sine model.

Table 6
Free vibration without an initial load

Mode n	Present ω (Hz)	Error (%)	Sine (Karama et al., 1993) ω (Hz)	Error (%)	Abaqus (Karama et al., 1993) ω (Hz)
1	14.958	0.06	14.96	0.09	14.95
2	57.796	0.34	57.866	0.46	57.60
3	123.396	0.49	123.696	0.73	122.80
4	205.647	0.71	206.419	1.09	204.20
5	299.105	0.84	300.593	1.35	296.60
6	399.659	0.87	402.062	1.48	396.20
7	504.518	0.78	507.956	1.47	500.60
8	611.909	0.59	616.420	1.33	608.30
9	720.773	0.32	726.316	1.09	718.50
10	830.501	−0.02	836.978	0.76	830.70
11	940.779	−0.39	948.037	0.37	944.50
12	1051.465	−0.81	1059.307	−0.07	1060.0

Vibration frequencies for a thin beam for the first 12 modes.

Table 7
Free vibration without an initial load

Mode n	Present ω (Hz)	Error (%)	Sine (Karama et al., 1993) ω (Hz)	Error (%)	Abaqus (Karama et al., 1993) ω (Hz)
1	83.050	0.18	83.698	−0.96	82.90
2	195.501	−2.54	195.730	2.43	200.60
3	317.232	−2.18	313.402	3.36	324.30
4	453.926	0.85	441.776	1.85	450.10
5	608.250	5.53	583.718	−1.27	576.40
6	780.830	11.10	740.575	−5.37	702.80
7	970.985	17.11	912.647	−10.08	829.10
8	1177.229	23.21	1099.501	−15.07	955.50

Vibration frequencies for a thick beam for the first 12 modes.

Problem 6. Free vibration with an initial load.

An initial load is added to study the influence of this initial constraint on the free vibration of Problem 5. This load has the same direction as the buckling study, but its value is lower than the first critical load. In this analytical resolution, the non-linear term defined in the buckling study is taken into account.

The system of equations deduced from the motion of equations (22):

$$\begin{aligned} \Gamma^{(u)} &= A_{11}u^{0*}_{1,11} - B_{11}w_{,111} + \widetilde{K}\phi_{1,11} \\ \Gamma^{(w)} &= B_{11}u^{0*}_{1,111} - D_{11}w_{,1111} + \widetilde{T}\phi_{1,111} + N^0_{11}w_{,11} \\ \Gamma^{(\phi)} &= \widetilde{K}u^{0*}_{1,11} - \widetilde{T}w_{,111} + \widetilde{S}\phi_{1,11} - \widetilde{Y}\phi_1 \end{aligned} \tag{50}$$

To determine the vibration frequency, using the Levy type solution equation (48), the determinant of the system of equation (50) is equal to zero:

$$\begin{bmatrix} I_w\omega^2 - \psi_n^2 A_{11} & I_{uw'}\psi_n\omega^2 + \psi_n^3 B_{11} & I_{u\omega}\omega^2 - \psi_n^2\widetilde{K} \\ I_{uw'}\psi_n^2\omega^2 + \psi_n^3 B_{11} & I_w\omega^2 + I_{w'}\psi_n^2\omega^2 - \psi_n^4 D_{11} - N^0_{11}\psi_n^2 & I_{\omega w'}\psi_n\omega^2 + \psi_n^3\widetilde{T} \\ I_{u\omega}\omega^2 - \psi_n^2\widetilde{K} & I_{\omega w'}\psi_n\omega^2 + \psi_n^3\widetilde{T} & I_\omega\omega^2 - \psi_n^2\widetilde{S} - \widetilde{Y} \end{bmatrix} \begin{pmatrix} U_n \\ W_n \\ \Phi_n \end{pmatrix} = 0 \tag{51}$$

Table 8
Free vibration with an initial load

Mode n	Present ω (Hz)	Error (%)	Sine (Karama et al., 1993) ω (Hz)	Error (%)	Abaqus (Karama et al., 1993) ω (Hz)
1	10.67	−0.12	10.67	−0.05	10.68
2	53.87	0.19	53.95	0.33	53.77
3	119.35	0.42	119.67	0.68	118.86
4	201.38	0.60	202.17	0.99	200.19
5	294.55	0.70	296.06	1.21	292.51
6	394.77	0.69	397.20	1.31	392.06
7	499.26	0.58	502.73	1.28	496.39
8	606.26	0.31	610.80	1.06	604.39
9	714.70	0.08	720.29	0.87	714.10
10	824.01	−0.26	830.53	0.53	826.16
11	933.84	−0.65	941.15	0.13	939.95
12	1044.09	−1.06	1051.97	−0.32	1055.30

Vibration frequencies for a thin beam for the first 12 modes.

So, now, for different values of n, different equations are obtained, in which the smallest positive root gives the vibration frequency of the associated mode n.

In the (Table 8), results are presented for the free vibration with an initial load (-10^7 N). For different modes of vibration, the frequencies are calculated using the present model. In the case of the thin beam, the maximum error found less than 0.75% with the present model, and 1.35% with the Sine model as far as the 11th mode of vibration, but after the 11th mode of vibration, the results are unfavourable with the present model.

4. Conclusion

The new multi-layered structure exponential model satisfies exactly and automatically the continuity condition of displacements and transverse shear stresses at interfaces, as well as the boundary conditions for a laminated composite with the help of the Heaviside step function (Figs. 1–7). For the new proposed model the results are compared with the existing model (Karama et al., 1993) like Sine model proposed by Touratier (1991) and by the finite element method by (Abaqus) (Karama et al., 1993). Results show that the new proposed exponential model is more precise or closer to finite element results than the Sine (Karama et al., 1993) model except for some results (Tables 1–8).

The new model is also simple in so far as any correction factor is used in opposition to the higher order models. The innovation in relation to the model proposed in the bibliography is also the introduction of the membrane refinement function $g(x_3)$, which represents the counterpart of the transverse shear function $f(x_3)$, which allows the x_3 to improve membrane refinement and then warping of the straight section in bending deformations (Table 1).

In the case of static analysis, (Tables 2–4) presents the numerical results for the bending deformation under different types of loading and boundary conditions on a thick beam, showing that the present model is much closer to the finite element analysis by Abaqus (Karama et al., 1993) than the Sine model (Karama et al., 1993). In (Figs. 1–8), different stresses and displacements are plotted with respect to the thickness and length for bending deformation, showing that the present model is still trying to approach the finite element results (Karama et al., 1993) much closely than the Sine model (Karama et al., 1993).

In the dynamic analysis, numerical results are more or less are favourable with the Abaqus reference.

As a whole we can conclude the present exponential model is more precise than other existing analytical models for multi-layered structures compared to finite element analysis.

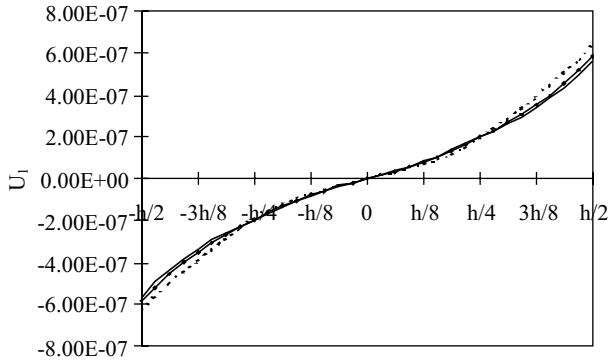

Fig. 8. Variation of the displacement U_1 through the thickness for $x_1 = L/4$ for Problem 2. Present (-∗-), Sine (Karama et al., 1993) (–), Abaqus (Karama et al., 1993) (- - -).

Appendix A. Virtual power of the acceleration quantities

We have,

$$\ddot{U}_1 = \ddot{u}_1^0 - x_3\ddot{w}_{,1} + h_1\ddot{\phi}_1, \quad \ddot{U}_3 = \ddot{w} \quad \text{and} \quad U_1^* = u_1^{0*} - x_3 w_{,1}^* + h_1\phi_1^*, \quad U_3^* = w^* \tag{A.1}$$

So Eq. (6) becomes,

$$P_{(a)}^* = \int_\Omega \rho(U_1^*\ddot{U}_1 + U_3^*\ddot{U}_3)\mathrm{d}\Omega \tag{A.2}$$

By the integration by parts:

$$P_{(a)}^* = \int_\Omega \rho[u_1^{0*}\ddot{u}_1 + (\ddot{u}_3 + x_3\ddot{u}_{1,1})w^* + h_1(x_3)\phi_1^*\ddot{u}_1]\mathrm{d}\Omega - \int_\Gamma \rho x_3 w^*\ddot{u}_1\,\mathrm{d}\Gamma \tag{A.3}$$

and, now:

$$\begin{aligned} P_{(a)}^* = \int_\Omega \rho\Big[&\Big(\ddot{u}_1^0 - x_3\ddot{w}_{,1} + h_1(x_3)\ddot{\phi}_1\Big)u_1^{0*} + \Big(\ddot{w} + x_3(\ddot{u}_{1,1}^0 - x_3\ddot{w}_{,11} + h_1(x_3)\ddot{\phi}_{1,1})\Big)w^* \\ &+ h_1(x_3)\Big(\ddot{u}_1^0 - x_3\ddot{w}_{,1} + h_1(x_3)\ddot{\phi}_1\Big)\phi_1^*\Big]\mathrm{d}\Omega - \int_\Gamma \rho x_3\Big(\ddot{u}_1^0 - x_3\ddot{w}_{,1} + h_1(x_3)\ddot{\phi}_1\Big)w^*\,\mathrm{d}\Gamma \end{aligned} \tag{A.4}$$

$$\begin{aligned} P_{(a)}^* = \int_0^L \Bigg[&\Bigg(\int_{-h/2}^{h/2}\rho\,\mathrm{d}x_3)\ddot{u}_1^0 + \int_{-h/2}^{h/2}(-\rho x_3\,\mathrm{d}x_3)\ddot{w}_{,1} + \int_{-h/2}^{h/2}(\rho h_1(x_3)\,\mathrm{d}x_3)\ddot{\phi}_1\Bigg)u_1^{0*} \\ &+ \Bigg(\int_{-h/2}^{h/2}\rho\,\mathrm{d}x_3)\ddot{w} + \int_{-h/2}^{h/2}(\rho x_3\,\mathrm{d}x_3)\ddot{u}_{1,1}^0 - \int_{-h/2}^{h/2}(\rho x_3^2\,\mathrm{d}x_3)\ddot{w}_{,11} + \int_{-h/2}^{h/2}(\rho x_3 h_1(x_3)\,\mathrm{d}x_3)\ddot{\phi}_{1,1}\Bigg)w^* \\ &+ \Bigg(\int_{-h/2}^{h/2}(\rho h_1(x_3)\,\mathrm{d}x_3)\ddot{u}_1^0 + \int_{-h/2}^{h/2}(-\rho x_3 h_1(x_3)\,\mathrm{d}x_3)\ddot{w}_{,1} + \int_{-h/2}^{h/2}(\rho h_1^2(x_3)\,\mathrm{d}x_3)\ddot{\phi}_1\Bigg)\phi_1^*\Bigg]\mathrm{d}\Omega \\ &+ \Bigg[\Bigg(\int_{-h/2}^{h/2}(-\rho x_3\,\mathrm{d}x_3)\ddot{u}_1^0 + \int_{-h/2}^{h/2}(\rho x_3^2\,\mathrm{d}x_3)\ddot{w}_{,1} + \int_{-h/2}^{h/2}(-\rho x_3 h_1(x_3)\,\mathrm{d}x_3)\ddot{\phi}_1\Bigg)w^*\Bigg] \end{aligned} \tag{A.5}$$

and now by relations (7),

$$P_{(a)}^* = \int_0^L \left(\Gamma^{(u)}u_1^{0*} + \Gamma^{(w)}w^* + \Gamma^{(\phi)}\phi_1^*\right)\mathrm{d}x_1 + \bar{\Gamma}^{(w)}w^* \tag{A.6}$$

Appendix B. Virtual power of the internal work

By relation (11), virtual power of the internal work (10) become:

$$P_{(i)}^* = -\int_\Omega \left[\Big(u_{1,1}^{0*} - x_3 w_{,11}^* + h_1(x_3)\phi_{1,1}^*\Big)\sigma_{11} + 2\left(\frac{1}{2}h_{1,3}(x_3)\phi_1^*\right)\sigma_{13}\right]\mathrm{d}\Omega \tag{B.1}$$

$$P_{(i)}^* = -\int_\Omega \Big(\sigma_{11}u_{1,1}^{0*} - x_3 w_{,11}^*\sigma_{11} + h_1(x_3)\sigma_{11}\phi_{1,1}^* + \sigma_{13}h_{1,3}(x_3)\phi_1^*\Big)\mathrm{d}\Omega \tag{B.2}$$

Now, by integrating each term by parts;

$$P^*_{(i)} = -\int_\Omega \left[-\sigma_{11,1}u_1^{0*} - x_3\sigma_{11,11}w^* - h_1(x_3)\sigma_{11,1}\phi_1^* + h_{1,3}(x_3)\sigma_{13}\phi_1^*\right]\mathrm{d}\Omega - \int_\Gamma \left[\sigma_{11}u_1^{0*} - x_3\sigma_{11}w^*_{,1} + x_3\sigma_{11,1}w^* + h_1(x_3)\sigma_{11}\phi_1^*\right]\mathrm{d}\Gamma \tag{B.3}$$

$$P^*_{(i)} = \int_0^L \left[\left(\int_{-h/2}^{h/2}\sigma_{11,1}\,\mathrm{d}x_3\right)u_1^{0*} + \left(\int_{-h/2}^{h/2}x_3\sigma_{11,11}\,\mathrm{d}x_3\right)w^* + \left(\int_{-h/2}^{h/2}h_1(x_3)\sigma_{11,1}\,\mathrm{d}x_3\right)\phi_1^* - \left(\int_{-h/2}^{h/2}h_{1,3}(x_3)\sigma_{13}\,\mathrm{d}x_3\right)\phi_1^*\right]\mathrm{d}x_1 + \left[-\left(\int_{-h/2}^{h/2}\sigma_{11}\,\mathrm{d}x_3\right)u_1^{0*} + \left(\int_{-h/2}^{h/2}x_3\sigma_{11}\,\mathrm{d}x_3\right)w^*_{,1} - \left(\int_{-h/2}^{h/2}x_3\sigma_{11,1}\,\mathrm{d}x_3\right)w^* - \left(\int_{-h/2}^{h/2}h_1(x_3)\sigma_{11}\,\mathrm{d}x_3\right)\phi_1^*\right] \tag{B.4}$$

Now by relations (12),

$$P^*_{(i)} = \int_0^L (N_{11,1}u_1^{0*} + M_{11,11}w^* + (P_{11,1} - P_{13})\phi_1^*)\mathrm{d}x_1 - N_{11}u_1^{0*} - M_{11,1}w^* + M_{11}w^*_{,1} - P_{11}\phi_1^* \tag{B.5}$$

Appendix C. Virtual power of the external loading

By relations (15), virtual power of external loading (14), becomes;

$$P^*_{(e)} = \int_\Omega \begin{bmatrix} U_1^* & 0 & U_3^*\end{bmatrix}\begin{bmatrix} f_1\\ f_2\\ f_3\end{bmatrix}\mathrm{d}\Omega + \int_\Gamma \begin{bmatrix} U_1^* & 0 & U_3^*\end{bmatrix}\begin{bmatrix} F_1\\ F_2\\ F_3\end{bmatrix}\mathrm{d}\Gamma \tag{C.1}$$

$$P^*_{(e)} = \int_\Omega (f_1U_1^* + f_3U_3^*)\mathrm{d}\Omega + \int_\Gamma (F_1U_1^* + F_3U_3^*)\mathrm{d}\Gamma \tag{C.2}$$

$$P^*_{(e)} = \int_\Omega (f_1u_1^{0*} - f_1x_3w^*_{,1} + h_1(x_3)f_1\phi_1^* + f_3w^*)\mathrm{d}\Omega + \int_\Gamma (F_1u_1^{0*} - F_1x_3w^*_{,1} + h_1(x_3)F_1\phi_1^* + F_3w^*)\mathrm{d}\Gamma \tag{C.3}$$

$$P^*_{(e)} = \int_0^L \left[\left(\int_{-h/2}^{h/2}f_1\,\mathrm{d}x_3\right)u_1^{0*} + \left(\int_{-h/2}^{h/2}f_3\,\mathrm{d}x_3 + \int_{-h/2}^{h/2}x_3f_{1,1}\,\mathrm{d}x_3\right)w^* + \left(\int_{-h/2}^{h/2}h_1(x_3)f_1\,\mathrm{d}x_3\right)\phi_1^*\right]\mathrm{d}x_1 + \left[\left(\int_{-h/2}^{h/2}F_1\,\mathrm{d}x_3\right)u_1^{0*} + \left(\int_{-h/2}^{h/2}F_3\,\mathrm{d}x_3 - \int_{-h/2}^{h/2}x_3f_1\,\mathrm{d}x_3\right)w^* + \left(\int_{-h/2}^{h/2}h_1(x_3)F_1\,\mathrm{d}x_3\right)\phi_1^* - \left(\int_{-h/2}^{h/2}x_3F_1\,\mathrm{d}x_3\right)w^*_{,1}\right] \tag{C.4}$$

and now by relation (15),

$$P^*_{(e)} = \int_0^L (\overline{n}_1u_1^{0*} + (\overline{n}_3 + \overline{m}_{1,1})w^* + \overline{p}_1\phi_1^*)\mathrm{d}x_1 + \overline{N}_1u_1^{0*}(\overline{N}_3 - \overline{m}_1)w^* - \overline{M}_1w^*_{,1} + \overline{P}_1\phi_1^* \tag{C.5}$$

References

Ambartsumian, S.A., 1958. On theory of bending plates. Izv. Otd. Tech. Nauk. AN SSSR 5, 69–77.
Beakou, A., 1991. Homogénéisation et Modélisation des Coques Composites Multicouches. Thesis ENSAM, Paris.
Di Sciuva, M., 1987. An improved shear deformation theory for moderately thick multi-layered anisotropic shells and plates. J. Appl. Mech., ASME 54, 589–596.
Di Sciuva, M., 1993. A general quadrilateral multi-layered plate element with continuous inter-laminar stresses. Comput. Struct. 47 (1), 91–105.
Gachon, H., 1980. Sur le Flambage des Plaques: Modèle de Calcul, Modèles Expérimentaux. Construction Métallique 4, 23–52.
He, L.H., 1994. A linear theory of laminated shells accounting for continuity of displacements and transverse shear stresses at layer interface. Int. J. Solids Struct. 31 (5), 613–627.
Idlbi, A., 1995. Comparaison de Théories de Plaque et Estimation de la Qualité des Solution dans la Zone Bord. Thesis, ENSAM, Paris.
Kaczkowski, Z., 1968. Plates. Statistical Calculations. Arkady, Warsaw.
Karama, M., Touratier, M., Idlbi, A., 1993. An evaluation of the edge solution for a higher-order laminated plate theory. Compos. Struct. 25, 495–502.
Karama, M., Abouharb, B., Mistou, S., Caperaa, S., 1998. Bending, buckling and free vibration of laminated composite with transverse shear stress continuity model. Compos. Part B 29B, 223–234.
Kirchhoff, G.J., 1850. Uber das gleichgewicht und die bewegung einer elastischen schreitbe. Reine Angew Math. 40, 51–58.
Levinson, M., 1980. An accurate simple theory of the statics and dynamics of elastic plates. Mech. Res. Commun. 7, 343–350.
Love, A.E.H., 1934. A treatise on the mathematical theory of elasticity, fourth ed. Cambridge University Press.
Mindlin, R.D., 1951. Influence of rotary inertia and shear on flexural motions of isotropic elastic plates. J. Appl. Mech., ASME 18, 31–38.
Murthy, M.V.V., 1981. An improved transverse shear deformation theory for laminated anisotropic plates, NASA Technical Paper.
Ossadzow, C., Muller, P., Touratier, M., 1995. Une théorie générale des coques composites multicouches. Actes du deuxième Colloque National en Calcul des Structures, Giens, France, pp. 263–268.
Pagano, N.J., 1970. Exact solution for rectangular bi-directional composites and sandwich plates. J. Compos. Mater. 4, 20–34.
Palardy, R.F., Palazotto, A.N., 1990. Buckling and vibration of the composite plates using the Levy method. Compos. Struct. 14, 61–85.
Panc, V., 1975. Theories of Elastic Plates. Academia, Prague.
Reddy, J.N., 1984. A simple high-order theory of laminated composite plate. J. Appl. Mech. 51, 745–752.
Reissner, E., 1945. Reflection on the theory of elastic plates. J. Appl. Mech. 38, 1453–1464.
Reissner, E., 1975. On transverse bending of plates, including the effects of transverse shear deformation. Int. J. Solid Struct. 25, 495–502.
Touratier, M., 1991. An efficient standard plate theory. Int. J. Engng. Sci. 29 (8), 901–916.
Touratier, M., 1992. A generalization of shear deformation theories for axisymmetric multi-layered shells. Int. J. Solids Struct. 29 (11), 1379–1399, A refined theory of laminated shallow shells. Int. J. Solids Struct. 29 (11), 1401–1415.
Widera, G.E.O., Logan, D.L., 1980. Refined theories for non-homogeneous anisotropic cylindrical shells: Part I and II. J. Engng. Mech. Div. EM6, 1053–1090.